

MIT Open Access Articles

The GlueX Experiment: First Results

The MIT Faculty has made this article openly available. **Please share** how this access benefits you. Your story matters.

Citation: Fanelli, Cristiano. "The GlueX Experiment: First Results." *Few-Body Systems* 58.3 (2017): n. pag.

As Published: <http://dx.doi.org/10.1007/s00601-017-1298-y>

Publisher: Springer Vienna

Persistent URL: <http://hdl.handle.net/1721.1/109608>

Version: Author's final manuscript: final author's manuscript post peer review, without publisher's formatting or copy editing

Terms of Use: Article is made available in accordance with the publisher's policy and may be subject to US copyright law. Please refer to the publisher's site for terms of use.



The GlueX experiment: first results

Cristiano Fanelli
(on behalf of the GlueX Collaboration)

Received: date / Accepted: date

Abstract GLUEX is a nuclear physics experiment located at the Thomas Jefferson National Accelerator Facility (JLab) designed to study and understand the nature of confinement in QCD by mapping the spectrum of exotic mesons. The experiment will be able to probe new areas by using photoproduction, i.e. the scattering on nucleon of ~ 9 GeV linearly polarized photons derived from the recently upgraded CEBAF with a 12 GeV electron beam. Spring 2016 has been characterized by a continued detector commissioning and initial running at the full design energy. The current status of the GLUEX detector performance and data collection will be discussed, with a brief overview of first physics results, future run plans, and long term upgrades.

Keywords GLUEX · confinement · QCD · first results

1 Introduction

The primary goal of the GLUEX experiment is to understand the nature of confinement in Quantum Chromodynamics (QCD) by studying the light meson spectrum and the properties of hybrid mesons for which the gluonic field would directly contribute to the J^{PC} quantum numbers [1].

Lattice QCD calculations suggest that several of the nonets of these hybrid mesons have exotic quantum numbers, corresponding to J^{PC} values forbidden for a simple fermion-antifermion system [2]. The expected masses for the lightest hybrids are suited to the energy and kinematics accessible to the GLUEX experiment, which is located in Hall D at the end of a new beamline from the Continuous Electron Beam Accelerator Facility (CEBAF) at Jefferson Lab (JLab), using 12 GeV electrons to deliver linearly-polarized photons. Here the

C. Fanelli
Massachusetts Institute of Technology, Laboratory for Nuclear Science, 77 Massachusetts Ave, Cambridge, MA 02139, USA
E-mail: cfanelli@mit.edu

photon beam impinges on a hydrogen target contained within a detector characterized by a near-complete charged and neutral particle coverage. In spring 2016, GLUEX has completed its commissioning and taken its first substantial data in the design configuration.

In this document we present some of the first results of the GLUEX experiment with 2016 data as well as an overview of the future physics program which will benefit from the next upgrade of the particle identification (PID) system with the addition of the DIRC detector.

2 The Beamline

The Hall D takes advantage of the 12 GeV electron beam from the upgraded CEBAF. The electrons pass through a bremsstrahlung radiator and then into the dipole magnet for tagging the energy of the scattered electrons (see Fig. 1 on the left). For the electrons producing a bremsstrahlung photon in the region between 25% and 98% of the primary electron beam energy, the scattered electrons are detected in a pair of tagger hodoscopes, hence tagging the energy of the photon. For 12 GeV/c electrons, the fine-grained *Tagger Microscope* (TAGM) has been placed to tag photons in the range between 8.2 GeV and 9.2 GeV, with each microscope element spanning 10 MeV in energy. For both higher and lower energy photons, the *Tagger Hodoscope* (TAGH) tags photons using elements about 30 MeV wide.

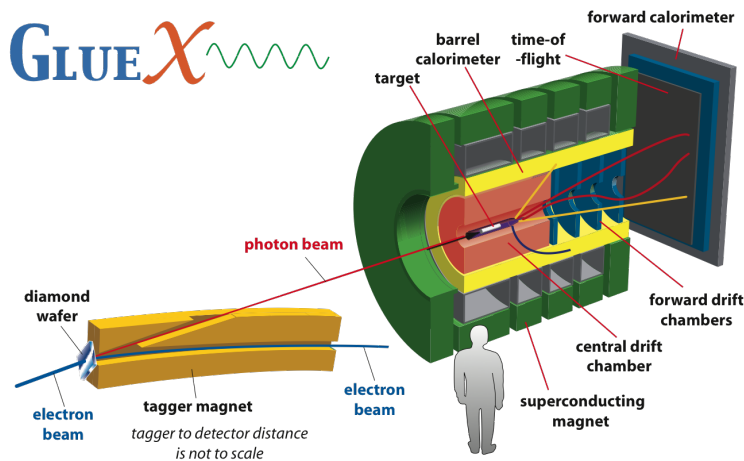


Fig. 1 A sketch of the photon tagger and the GLUEX detector at JLab.

A $20\ \mu\text{m}$ diamond crystal is utilized as a radiator to produce a linearly polarized coherent bremsstrahlung photon beam. The photons in the coherent peak range from 8.4 GeV to 9 GeV and are linearly polarized relative to the crystal axes in the diamond with an expected polarization of $\sim 40\%$.

The diamond can be rotated to produce two perpendicular directions of the polarization. The photons travel through an 80 m long vacuum beamline before entering Hall D. Since the coherent bremsstrahlung photons are produced in the direction of the incident electrons, while the incoherent bremsstrahlung photons are produced within a cone around this direction, the off-axis photons are removed by passing the beam through a 3.4 mm diameter collimator. The photons pass then through a *Triplet Polarimeter* which is used to monitor the linear polarization, an information needed in the measurements of the beam asymmetry as explained in the following. Successively they enter a *Pair Spectrometer* system [3] that is used to monitor both the energy and intensity of the beam. Finally the photons reach the GLUEX spectrometer to impinge on the liquid hydrogen target to produce the physics events that will be detected. The initial operation of GLUEX was with beam intensity of 10^7 γ/s in the coherent peak. The ultimate rate is expected to be an order of magnitude higher.

3 The GlueX Detector and PID upgrade

The GLUEX detector is represented schematically on the right part of Fig. 1. It is characterized by a near uniform acceptance for both charged and neutral particles in the polar angle range from 1° to 120° . The 30 cm long liquid hydrogen target is located in the barrel part of the detector. The solenoid magnet provides a magnetic field of about 2 T along the direction of the beam.

Particles produced in the interaction are first detected by a scintillator-based *Start Counter* surrounding the target and the beamline in the forward direction. The *Central Drift Chamber* (CDC) [4] based on straw-tube technology immediately surrounds the start counter and provides the position measurement along the charged tracks with $150 \mu\text{m}$ accuracy in the $r - \phi$ plane and at the mm level along the beam axis. It also provides a measurement of dE/dx for charged tracks which allows to separate π/p up to a momentum of 1 GeV/c. The *Forward Drift Chamber* (FDC) [5] complements the tracking system in the forward region and performs PID by measuring dE/dx . The *Barrel Calorimeter* (BCAL) [6,7] surrounds the tracking devices inside the solenoid and covers the polar angle acceptance between 11° and 120° . The energy resolution is $\sigma_E/E \approx 6\%/\sqrt{E} \oplus 2\%$. The timing information is used to provide time-of-flight for particles interacting in the BCAL contributing to the global PID for both charged particles and photons. The *Forward Calorimeter* (FCAL) [8] is located downstream of the solenoid magnet to cover a range in polar angles between 1° and 11° . FCAL is sensitive to photons with energy above 100 MeV and has a similar energy resolution to BCAL. The *Time-Of-Flight* (TOF) wall located upstream of FCAL comprises two layers of scintillator bars which are read out on both sides using photomultiplier tubes. The TOF contributes to the PID of forward going particles by providing the timing and energy-loss information, with a timing resolution of 100 ps. All of the detector systems are now performing near the design specifications.

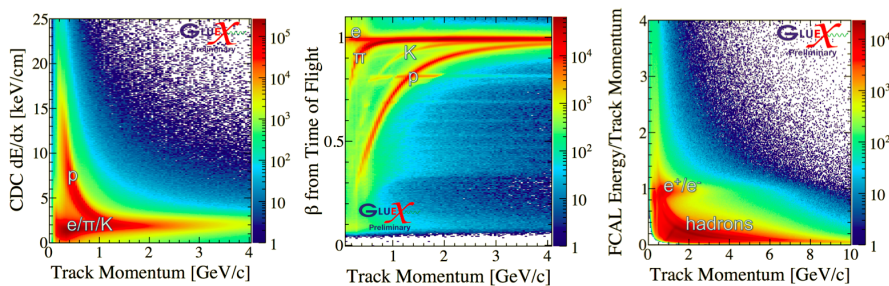


Fig. 2 (left) Energy loss dE/dx in the CDC (middle) β as determined from TOF and (right) the energy measured by the FCAL divided by the momentum of the associated track. All these quantities are shown as a function of the reconstructed momentum of the track.

An example of the PID capabilities are shown in Fig. 2 for CDC, TOF, and FCAL respectively, as a function of the particle momentum. The energy loss in CDC (Fig. 2 (left)) allows to separate the proton from the other positively charged particles up to 1 GeV/c. The TOF β (Fig. 2 (middle)) is characterized by clear bands for π^+ , K^+ , e^+ , and p, with a distinguishable proton up to 3 GeV/c and effective π/K separation up to about 2 GeV/c. Fig. 2 (right) shows the ratio of the energy deposited in FCAL normalized to the associated track momentum as a function of the track momentum. This quantity allows to separate electrons/positrons ($E/p \sim 1$) from hadrons in the FCAL.

Different types of measurements are planned to take advantage of the potential of the GLUEX detector. The physics program began in 2016, the first data being already sufficient to measure the beam asymmetry for several photo-produced reactions (e.g. $\gamma p \rightarrow pX$, $X = \pi, \eta, \eta', \rho, \omega, \phi$), as reported briefly in the following section. The physics data from 2017 and 2018 (planned at low intensity with 10 MHz in the peak) will allow to measure cross sections, spin-density matrix elements, as well as the start of the exotic hybrids search and the partial wave analysis program. The GLUEX strangeness program complements the mapping of the hybrid spectrum by identifying final states with kaons. In particular, the quark flavor composition of a meson can be experimentally inferred by comparing the branching ratios for strange and non-strange decays. A systematic study of the kaon final states is planned for 2018 after the upgrade of the PID system.

A new DIRC (*Detection of Internally Reflected Cherenkov light*) detector [9] will be installed in the forward region of the spectrometer. After the installation is completed, GLUEX will run in a high intensity mode (50 MHz in the peak) focusing on the identification of states with hidden strangeness and hyperon resonances. The four existing BaBar DIRC [10] bar boxes filled with long and narrow radiators ($1.75 \times 3.5 \times 490 \text{ cm}^3$) will be reused in the GLUEX DIRC without any modifications. Each pair of boxes will be attached to a new compact photon camera, inspired by [11]. Further details on the DIRC design can be found in [12,13]. The GLUEX DIRC is located about 4 m away from the target and forms a thin wall of fused silica radiators attached to photon

cameras read-out by an array of multi-anode photomultipliers (MaPMT). The DIRC will cover the polar angle range from 2° to 11° and requires four unaltered BaBar bar boxes each made of 12 radiators. The bar boxes will be oriented horizontally and installed upstream of the TOF detector, with two bar boxes above and two below the beam and each pair attached to a photon camera (one of which located to the left, the other to the right of the beam respectively). The construction has been started, and the calibration system is being studied. The GLUEX DIRC will provide a clean separation between π/K of at least 3σ for momenta less than 4 GeV/c.

4 Preliminary results

The primary goal of the GLUEX experiment is to search for and ultimately map out the spectrum of light quark hybrid mesons using partial wave analysis. In the next years the beam intensity will be increased to cover all parts of the GLUEX exotic hybrid program. An extensive research program complements and enhances these physics goals. This ranges from studies of photo-produced resonances to physics beyond the Standard Model. The first data collected in Spring 2016 allowed for several physics opportunities (most of which shown at DNP, Vancouver 2016). Part of these topics is briefly reported in what follows.

Early Spectroscopy and Asymmetries: The beam asymmetry Σ provides insight into the dominant production mechanism [14], whose understanding is crucial to disentangle the J^{PC} of observed states in the exotic hybrid search. GLUEX has measured the photon beam asymmetry for the reactions $\gamma p \rightarrow \pi^0 p$ and $\gamma p \rightarrow \eta p$ [15] using the 9 GeV linearly-polarized, tagged photon beam incident on a liquid hydrogen target. It's worth mentioning that the asymmetries, measured as a function of the proton momentum transfer, possess greater precision than previous π^0 measurements, and are the first η measurements in this energy regime. The photon beam linear polarization is measured using the Triplet Polarimeter, with the azimuthal angle of the beam photon's linear polarization plane in two configurations, PARA ($\phi_\gamma^{lin} = 0^\circ$) and PERP ($\phi_\gamma^{lin} = 90^\circ$). Σ is extracted as the only free parameter of the fit of the yield asymmetry defined by combining the two perpendicular configurations as a function of the azimuthal angle of the production plane defined by the final state proton, ϕ_p , as shown in Fig. 3. The results on the asymmetry are compared to existing theoretical predictions based on t-channel, quasi-particle exchange [16, 17, 18], and are thus expected to contribute to our comprehension of the production mechanism in photo-production at high energy.

Transition Form Factors: Radiative decays of mesons are powerful probes of the hadron structure. The GLUEX experiment will produce and record huge samples of light mesons, opening the possibility to study their radiative decays and to measure the transition form factors of the η and η' mesons [19].

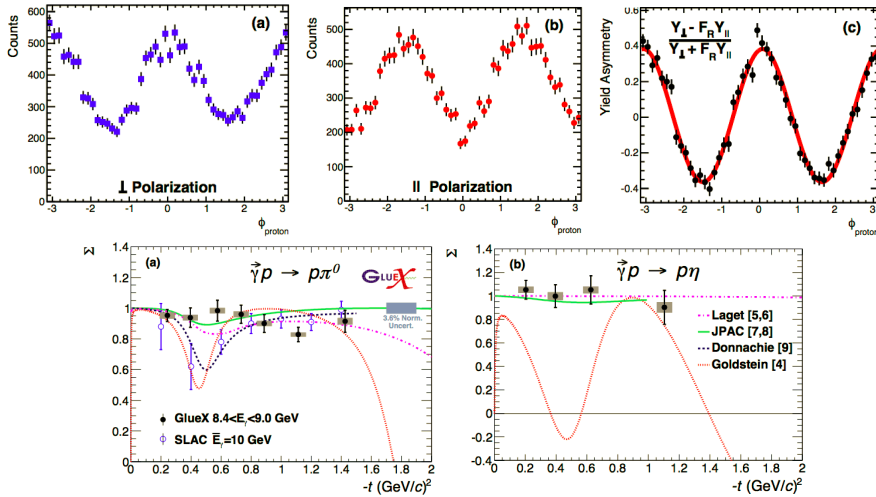


Fig. 3 (top) $\gamma p \rightarrow \pi^0 p$ yield versus ϕ_p integrated over $-t$ for (a) PERP and (b) PARA. (c) The yield asymmetry to extract the beam asymmetry Σ . (bottom) (a) Σ for $\gamma p \rightarrow \pi^0 p$ and (b) $\gamma p \rightarrow \eta p$. See for more details [15].

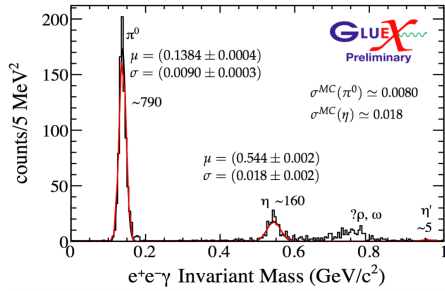


Fig. 4 $M(e^+e^-\gamma)$ invariant mass from the process $\gamma p \rightarrow p e^+ e^- \gamma$ with part of the data collected in 2016 at GLUEX, corresponding approximately to 1% of the total integrated luminosity that will be collected in the next years (cf. ‘Phase IV’).

measure the pseudo-scalar meson radius, whose physical interpretation has still not completely been explored by the theory. A recent study [21] including first results with real data suggests that GLUEX will be competitive in the next years with the current experimental results of the $\eta(\prime)$ TFF’s measurements [22,23]. A preliminary plot of the invariant mass distribution in the $e^+e^-\gamma$ channel is shown in Fig. 4.

Physics Beyond the Standard Model: Dark Matter (DM) dominates the matter density in the universe, but very little is known about it. Its existence and stability provides a strong hint that there may be a dark sector,

The TFF’s are important in studies of the muon anomalous magnetic moment, $a_\mu = (g_\mu - 2)/2$, since the hadronic light-by-light (HLbL) scattering contribution to a_μ includes two meson-photon-photon vertices that can be related to the form factors in $P \rightarrow \gamma\gamma^* \rightarrow \gamma e^+ e^-$ decays [20]. Models describing these transitions should be tested as precisely as possible to reduce the uncertainty in the SM prediction for a_μ . The low Q^2 slope of the TFF provides a unique method to measure

which consists of a rich symmetry structure with new forces and new particles not interacting by the known forces (with the exception of gravity). Consequently, the discovery of these particles would have a profound impact in our understanding of the universe. There are only a few well-motivated interactions that provide a “portal” from the SM sector into the dark sector [24], among these the dark vector portal has inspired a global effort at high intensity frontier centers at intermediate energies like Jefferson Lab. A compelling dark-force scenario consist of promoting the baryon number to a gauge symmetry $U(1)_B$, in this way extending the SM to produce new bosons with direct coupling to quarks and not to leptons (viz. “leptophobic B bosons”).

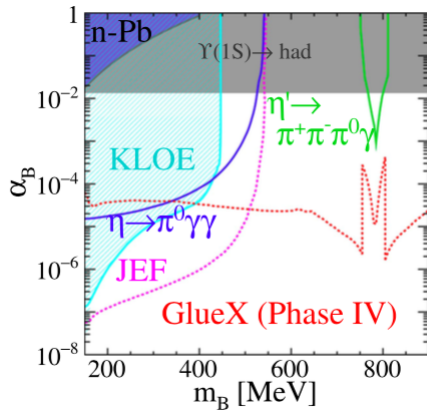


Fig. 5 Existing limits on B bosons compared to the expected sensitivity obtained from η decays at JEF [26] and photoproduction [25].

If $U(1)_B$ is broken, B is a massive vector boson with quark couplings. This B boson has $I^G(J^{PC}) = (0^-)1^{--}$, similarly to ω and ϕ . Recently the direct photoproduction of leptophobic bosons that couple to quarks has been calculated [25] and it has been estimated that $\gamma p \rightarrow pB$ will provide the best sensitivity for B masses above 0.5 GeV, as shown in Fig. 5. GLUEX will discover or tightly constrain the existence of a directly photo-produced B boson in this mass range. Preliminary results based on 2016 data and scaled to the higher integrated luminosity of GLUEX Phase IV

are consistent with these predictions [27].

5 Summary

The GLUEX experiment has been successfully commissioned, and the first analyses based on the available data are in progress. This paper in section 4 reports on some of the first physics results obtained: (i) early spectroscopy and the beam asymmetry measurements [15], (ii) transition form factors with radiative decay studies showing encouraging results and (iii) beyond Standard Model searches with scaled preliminary results consistent with predictions.

The first stage of GLUEX running at low intensity (10 MHz in the peak) is dedicated mainly to measurements of cross-sections, asymmetries, and spin-density matrix elements, along with the identification of known resonances and hybrids using partial wave analysis. After 2018 it is planned to increase the beam intensity by a factor of 5 to cover all parts of the GLUEX exotic hybrid program and upgrade the PID system by installing the DIRC detector.

References

1. C. A. Meyer and E.S. Swanson, *Prog. Part. Nucl. Phys.* **82**, 21-58 (2015).
2. J. J. Dudek *et al.*, *Phys. Rev. D* **88**, no. 9, 094505 (2013). [arXiv:1309.2608 [hep-lat]].
3. F. Barbosa *et al.*, *Nucl. Instrum. Meth. A* **795**, 376 (2015).
4. Y. Van Haarlem *et al.*, *Nucl. Instrum. Meth. A* **622**, 142 (2010). [arXiv:1004.3796 [nucl-ex]].
5. Berdnikov, V. V. *et al.*, *Instr. Exp. Tech.* **58**, 25 (2015).
6. Z. Papandreou *et al.*, *Nucl. Instrum. Meth. A*, **596**, 338 (2008).
7. A.E. Baulin *et al.*, *Nucl. Instrum. Meth. A*, **715**, 48 (2013).
8. K. Moriya *et al.*, *Nucl. Instrum. Meth. A*, **726**, 60 (2013).
9. J. Stevens *et al.*, *JINST* **11**, no. 07, C07010 (2016). [arXiv:1606.05645 [physics.ins-det]].
10. I. Adam *et al.*, *Nucl. Inst. Meth. A* **538**, 281 (2005).
11. B. Dey *et al.*, *Nucl. Instrum. Meth. A* **775**, 112 (2015). [arXiv:1410.0075 [physics.ins-det]].
12. GlueX Collaboration, GlueX DIRC Technical Design Report (2015). Available at: https://halldweb.jlab.org/DocDB/0028/002809/003/dirc_tdr.pdf
13. J. Hardin and M. Williams, *JINST* **11** no. 10, P10007 (2016).
14. I. S. Barker, A. Donnachie, and J. K. Storrow, *Nucl. Phys.* **B95**, 347 (1975).
15. H. Al Ghouh *et al.* (GlueX Collaboration), arXiv:1701.08123 (2017).
16. J. M. Laget, *Phys. Lett.* **B695**, 199 (2011).
17. V. Mathieu, G. Fox, and A. P. Szczepaniak, *Phys. Rev.* **D92**, 074013 (2015).
18. A. Donnachie and Yu. S. Kalashnikova, *Phys. Rev.* **C93**, 025203 (2016).
19. A. M. Bernstein, PoS CD15 (2016) 046 SISSA (2016-02-26).
20. T. Blum *et al.*, *The Muon (g-2) Theory Value: Present and Future* (2013). Available at: <https://arxiv.org/abs/1311.2198>
21. C. Fanelli and M. Williams (GlueX Collaboration), Study of the $\eta(\prime) \rightarrow e^+e^-\gamma$ decay at GlueX and Transition Form Factors. APS Division of Nuclear Physics Vancouver Meeting (2016).
22. Aguar-Bartolome *et al.*, *Phys. Rev. C* **89**, 044608 (2014).
23. M. Ablikim *et al.* (BESIII Collaboration), *Phys. Rev. D* **92**, 012001 (2015).
24. R. Essig *et al.*, Dark sectors and new, light, weakly-coupled particles (2013). Available at: <https://arxiv.org/abs/1311.0029>
25. C. Fanelli and M. Williams, *J. Phys. G* **44**, 1, 014002 (2016).
26. The GlueX Collaboration and Other Participants, JLab proposal PR12-14-004 (2014). Available at: https://www.jlab.org/exp_prog/proposals/14/PR12-14-004.pdf
27. J. Hardin, C. Fanelli and M. Williams (GlueX Collaboration), Leptophobic Boson Searches. APS Division of Nuclear Physics Vancouver Meeting (2016).